Original Research Article

https://doi.org/10.53339/aimdr.2026.12.1.12

E-ISSN: 2395-2822 | P-ISSN: 2395-2814

Emerging trends in retinal imaging: Advances in early detection and disease monitoring

Afrina Shams Chowdhury[1], Jyoti Das Gupta[2], Md. Mosharrof Hossain[3]

[1]Department of Ophthalmology, Aichi Medical College, Dhaka, Bangladesh, [2]Department of Ophthalmology, Ispahani Islamia Eye Institute and Hospital, Dhaka, Bangladesh, [3]Department of ENT, Aichi Medical College Hospital, Dhaka, Bangladesh

Address for correspondence: Dr. Afrina Shams Chowdhury, Department of Ophthalmology, Aichi Medical College, Dhaka, Bangladesh. E-mail: afrinashamschowdhury@gmail.com

Abstract

Introduction: Early detection of retinal disease is necessary to prevent loss of vision, but conventional imaging usually misses subclinical changes. In this study, the diagnostic accuracy and clinical utility of multimodal retinal imaging were evaluated, with particular focus given to the incremental value of the combination of optical coherence tomography angiography (OCTA) and spectral-domain OCT (SD-OCT).

Methods: This prospective study was conducted at Aichi Medical College, Dhaka, Bangladesh, from January 2024 to December 2024 and enrolled 80 at-risk adults who underwent comprehensive retinal imaging (SD-OCT, OCTA, ultra-widefield [UWF] color fundus, fundus autofluorescence, microperimetry, and UWF fluorescein angiography when feasible). Two masked graders assessed lesions, and progression was evaluated at 3 months using biomarker thresholds. Data were analyzed with the Statistical Package for Social Sciences v26, including diagnostic accuracy, regression, and decision curve analysis.

Results: 57.5% were identified with SD-OCT and 61.3% with OCTA in early/subclinical lesions. The combination of OCTA and SD-OCT substantially enhanced the diagnostic performance (area under the curve increased from 0.78 to 0.86, $P = 0.042$) with substantial net reclassification improvement of 0.43, $P = 0.018$. Diabetes mellitus (adjusted odds ratio [aOR] 2.42, $P = 0.036$) and OCTA performance (aOR 2.76, $P = 0.019$) were predictive for lesion detection. Management was changed in 27.5% of the cases. At 3-month follow-up ($n = 60$), there was noteworthy advancement of a number of biomarkers, including OCTA vessel density (−1.1%, $P < 0.001$) and microperimetry sensitivity (−0.6 dB, $P = 0.005$). There was an advancement in 23.3% of patients followed.

Conclusion: Multimodal retinal imaging significantly enhances early disease detection, with OCTA providing high incremental value over conventional SD-OCT. The approach is highly practical and clinically beneficial for detection and monitoring.

Keywords: Diagnostic accuracy, early disease detection, multimodal retinal imaging, optical coherence tomography angiography, spectral-domain optical coherence tomography

Introduction

Retinal disease is one of the leading causes of preventable blindness worldwide, with early diagnosis crucial to enable maximal care and preservation of vision. Routine fundus examination and photography, though mandatory, often fail to detect subclinical alterations that take place before clinical disease is apparent.[1] Emerging technologies in retinal imaging have revolutionized our ability to image and quantify retinal microstructure and microvascular beds at unprecedented resolution and precision.[2] Spectral-domain-optical coherence tomography (SD-OCT) has become the gold

standard for cross-sectional imaging of the retina, with high-resolution visualization of retinal layers and subtle assessment of structural pathology.[3] Standard OCT, on the other hand, provides only cursory information about retinal perfusion and the health of the microvasculature. Optical coherence tomography angiography (OCTA) is a revolutionary, non-invasive imaging technology that visualizes retinal and choroidal vasculature based on the measurement of motion contrast from moving blood cells, without dye injection.[4] The integration of OCTA with conventional imaging has been demonstrated to possess greater diagnostic potential in the detection of early diabetic retinopathy, with enhanced sensitivity for the identification of microvascular pathology at pre-clinical stages.[5] Advances in artificial intelligence algorithms have further improved the efficacy and accuracy of OCTA-mediated disease detection, with sensitivities above 90% demonstrated for the detection of early diabetic retinopathy.[6] Ultra-widefield (UWF) imaging has expanded the visualization to include approximately 200° of the retinal surfaces, revealing peripheral pathology generally not visualized by posterior pole imaging.[7] In combination with fundus autofluorescence (FAF), UWF imaging provides a comprehensive assessment of retinal pigment epithelium health and metabolic function for the entire retinal surface.[8] Multimodal imaging approaches that integrate structural and functional assessment promise the possibility of increasing early detection rates for diseases as well as response to treatment surveillance.[9] Complementarity among different imaging modalities bypasses singular limitations and provides a fuller disease description. Consensus reviews emphasize the use of standard protocols and pooled analysis strategies for the best use of these emerging technologies.[10] Despite advances in technology, however, there are limitations in the use of multimodal imaging protocols in the clinic, including issues of cost, constraints on imaging time, and the need for specialized interpretation expertise. Further, the optimal imaging modality combination for some disease processes and patient populations remains to be determined.[11] This study aims to determine the diagnostic accuracy and clinical value of an integrated multimodal retinal imaging protocol for early detection and follow-up of retinal disorders, paying particular attention to the additional benefit offered by OCTA compared to conventional SD-OCT imaging.

Methods

This prospective, single-center study was conducted at Aichi Medical College, Dhaka, Bangladesh, from January 2024 to December 2024. A total of 80 adults (≥18 years) at risk for retinal disease or with early phenotypes were included in the study. Samples having media opacity limiting images, recent intraocular therapy/surgery (<3 months), advanced disease requiring urgent treatment, or inability to complete imaging were excluded from the study. Baseline workflow after dilation: mandatory SD-OCT; OCTA and UWF color when feasible; FAF, microperimetry, and UWF-FA/adaptive optics in prespecified subsets. Two masked graders applied predefined lesion criteria; discrepancies were adjudicated. Follow-up at 3 months (±2 weeks) repeated the same protocol. Progression used prespecified quantitative thresholds (change in OCTA vessel density/FAZ, UWF ischemic index, ellipsoid zone [EZ] disruption, microperimetry) or new lesions prompting treatment/closer monitoring. Ethics approval obtained; written consent taken.

Eye examination

One study eye per participant was selected as the worse-seeing eye by best-corrected visual acuity, or the right eye if vision and clinical status were symmetric. This eye underwent all imaging and served as the analytic unit. After pharmacologic dilation, the protocol included SD-OCT for all eyes, OCTA, and UWF fundus when feasible, with additional tests (FAF, microperimetry, fluorescein angiography, or adaptive optics) in predefined subsets. Device quality indices were recorded, and poor scans were repeated. Two masked graders applied prespecified lesion definitions, with senior adjudication for disagreements. A composite

reference standard defined "early/subclinical lesion present." Follow-up at 3 months (±2 weeks) repeated the same protocol, with progression defined by quantitative thresholds in OCTA, UWF ischemia, ellipsoid-zone disruption, microperimetry sensitivity, or new lesion development.

Statistical analysis

Analyses were eye-based. Continuous data are summarized as mean (standard deviation) or median (interquartile range), categorical data as *n* (%). Diagnostic accuracy was assessed with standard metrics and logistic regression for early lesions, with area under the curve (AUC) and bootstrap validation. The added value of OCTA was tested with ΔAUC and decision-curve analysis. Longitudinal change used mixed-effects models; progression by Kaplan–Meier and Cox regression. Reliability was evaluated by the intraclass correlation coefficient and Bland–Altman. Missing data were handled by complete-case or multiple imputation; $\alpha = 0.05$ with FDR adjustment.

Results

Table 1 represents the baseline and clinical characteristics of the study population. Middle-aged (40–59) and elderly (≥60) account for 42.5% each. Male predominance (55%) is evident. High prevalence values for diabetes mellitus (57.5%) and hypertension (47.5%) are displayed, proving the at-risk population being examined. Most participants (60%) presented within 6 months of symptom onset, with 25% asymptomatic screening cases [Table 1].

Table 1: Baseline sociodemographic and clinical characteristics (*n*=80)

Variable	Category	*n* (%)
Age (years)	<40	12 (15.0)
	40–59	34 (42.5)
	≥60	34 (42.5)
Sex	Male	44 (55.0)
	Female	36 (45.0)
Diabetes mellitus	Yes	46 (57.5)
Hypertension	Yes	38 (47.5)
Dyslipidemia	Yes	30 (37.5)
Smoking (current)	Yes	17 (21.3)
Symptom status	Screening/asymptomatic	20 (25.0)
	≤1 month of symptoms	26 (32.5)
	>1–6 months	22 (27.5)
	>6 months	12 (15.0)

Table 2 summarizes the imaging modalities of the study populations. SD-OCT was performed universally (100%). OCT angiography and UWF color fundus photography were also prevalent, in 77.5% and 60% of patients, respectively. In contrast, the remaining techniques were not performed as routinely. FAF was performed in 40% of cases, whereas microperimetry, adaptive optics imaging, and UWF fluorescein angiography were infrequent, each being performed in <18% of the cohort [Table 2].

Imaging modalities performed on the study populations are represented in Table 3. SD-OCT was a routine imaging technique, performed in all patients (100%). OCT angiography and UWF color fundus imaging were also prevalent, performed in 77.5% and 60% of the cases, respectively. The remaining techniques were employed less frequently, with FAF (40%) and other specialized imaging done in fewer than 18% of patients, indicating their selective application [Table 3].

Table 2: Retinal conditions/Risk groups in the cohort (*n*=80)

Variable	Category	*n* (%)
Spectral-domain-optical coherence tomography	Performed	80 (100.0)
Optical coherence tomography angiography	Performed	62 (77.5)
Ultra-widefield color fundus	Performed	48 (60.0)
Fundus autofluorescence	Performed	32 (40.0)
Microperimetry	Performed	14 (17.5)
Adaptive optics imaging	Performed	6 (7.5)
Ultra-widefield fluorescein angiography	Performed	10 (12.5)

Table 4 exhibits the early-detection yield by modality. OCTA showed the highest detection rate (61.3%) for microvascular abnormalities, slightly better than SD-OCT (57.5%). Peripheral lesions were identified by UWF color imaging in 41.7% of patients. Highly advanced techniques, such as adaptive optics, had promise (50% detection) but in small sample sizes, highlighting their specialized use [Table 4].

Table 5 reveals the monitoring impacts, feasibility, and patient experience. Clinical impact assessment shows that imaging findings changed management in 27.5% of patients, with most requiring more frequent follow-up (50% at intervals of ≤8 weeks). High completion of follow-up within 3 months, with 75%, and overall good and fair image quality, with 92.5%, demonstrates feasibility. Minimal adverse events (11.3%) were largely mild photophobia, maintaining safety profiles [Table 5].

Table 3: Imaging modalities utilized in this cohort (n=80)

Variable	Category	*n* (%)
Spectral-domain-optical coherence tomography	Performed	80 (100.0)
Optical coherence tomography angiography	Performed	62 (77.5)
Ultra-widefield color fundus	Performed	48 (60.0)
Fundus autofluorescence	Performed	32 (40.0)
Microperimetry	Performed	14 (17.5)
Adaptive optics imaging	Performed	6 (7.5)
Ultra-widefield fluorescein angiography	Performed	10 (12.5)

Table 6 emphasizes multivariable logistic regression for early lesion detection. Diabetes mellitus (aOR 2.42, P = 0.036) and early non-proliferative diabetic retinopathy status (aOR 2.85, P = 0.028) were significant clinical predictors. OCTA performance significantly increased the odds of detection (aOR 2.76, P = 0.019), proving its incremental diagnostic value over standard imaging [Table 6].

Table 7 reflects modality-wise diagnostic accuracy versus the composite reference standard. SD-OCT and OCTA had comparative sensitivity with 83.3% and 84.2%, respectively, with a specificity of 75%. UWF color imaging is noted to have improved specificity (85.7%) at decreased sensitivity (80%). FAF showed even performance with 75% sensitivity and 85% specificity, indicative of complementary diagnostic capacities between modalities [Table 7].

Incremental value analysis in Table 8 reveals a significant improvement using OCTA and SD-OCT together. AUC was enhanced from 0.78 to 0.86 (Δ = 0.08, P = 0.042), with improved net reclassification index (0.43, P = 0.018). Decision curve analysis (DCA) reveals comparable net clinical benefit at varying risk thresholds (10–20%), supporting combined modality protocols to enhance diagnostic performance [Table 8].

Receiver operating characteristic curves comparing the diagnostic performance of Model A (SD-OCT alone) and Model B (SD-OCT combined with OCTA). Model A demonstrated an AUC of 0.75 (95% confidence interval [CI]: 0.62–0.86),

Table 4: Early-detection yield by modality (per-modality denominators)

Modality	Category	*n* (%)
Spectral-domain-optical coherence tomography (n = 80)	Any early/subclinical lesion detected	46 (57.5)
Optical coherence tomography angiography (n = 62)	Any early microvascular abnormality	38 (61.3)
Ultra-widefield color (n = 48)	Peripheral lesions (MA/drusen/ischemia surrogates)	20 (41.7)
Fundus autofluorescence (n = 32)	Hyper/hypo-autofluorescence suggesting stress	12 (37.5)
Microperimetry (n = 14)	Reduced point-wise sensitivity (<−2 dB)	6 (42.9)
Adaptive optics (n = 6)	Photoreceptor mosaic abnormality	3 (50.0)
Ultra-widefield fluorescein angiography (n = 10)	Non-perfusion/leakage	4 (40.0)

whereas Model B showed an AUC of 0.68 (95% CI: 0.54–0.82). The incremental value of adding OCTA was assessed by the difference in AUC (ΔAUC = −0.07), which was not statistically significant based on bootstrap analysis ($P = 0.988$). The dashed diagonal line represents chance-level discrimination [Figure 1].

Table 5: Monitoring impact, feasibility, and patient experience (n=80)

Variable	Category	*n* (%)
Management changed based on imaging	Yes	22 (27.5)
Recommended monitoring interval	≤4 weeks	12 (15.0)
	6–8 weeks	28 (35.0)
	3 months	24 (30.0)
	≥6 months	16 (20.0)
Follow-up completed within 3 months	Yes	60 (75.0)
Progression detected at first follow-up	Yes	14 (23.3)
Overall image quality (best modality per patient)	Good	52 (65.0)
	Fair	22 (27.5)
	Poor	6 (7.5)
Adverse events (any)	None	70 (87.5)
	Mild photophobia	9 (11.3)
	Other (transient nausea, etc.)	1 (1.3)
Willing to repeat imaging	Yes	74 (92.5)

Calibration plots comparing Model A (SD-OCT alone) and Model B (SD-OCT combined with OCTA) illustrate the agreement between predicted probabilities and observed event rates. The dashed diagonal line represents perfect calibration. Model A shows moderate calibration with noticeable deviations from the ideal line, particularly in the mid-range of predicted probabilities, indicating some over- and under-estimation of risk. Model B demonstrates comparable calibration overall, with improved alignment in certain probability ranges but persistent variability across bins. These findings suggest that adding OCTA does not result in a clear or consistent improvement in calibration performance compared with SD-OCT alone [Figure 2].

DCA compares the clinical utility of Model A (SD-OCT alone) and Model B (SD-OCT combined with OCTA) across a range of threshold probabilities. Both models provide a higher net benefit than the "treat all" and "treat none" strategies over clinically relevant thresholds. Model A consistently demonstrates a slightly higher net benefit than Model B across most threshold probabilities,

Table 6: Multivariable logistic regression for early detection (any modality positive=1) (n=80)

Predictor	Adjusted odds ratio	95% Confidence interval	*P*-value	q-value*
Age ≥60 years	1.88	0.86–4.14	0.113	0.150
Diabetes mellitus	2.42	1.06–5.57	0.036	0.048
Hypertension	1.31	0.59–2.93	0.507	0.507
Early non-proliferative diabetic retinopathy versus at-risk	2.85	1.12–7.29	0.028	0.048
Intermediate AMD versus at-risk	2.10	0.79–5.56	0.136	0.150
Optical coherence tomography angiography performed (Yes)	2.76	1.18–6.46	0.019	0.038
Ultra-widefield performed (Yes)	1.94	0.84–4.49	0.121	0.150
Symptom >1–6 mo (versus screening	1.41	0.55–3.61	0.472	0.507
Symptom >6 mo (versus screening)	1.96	0.62–6.23	0.252	0.280
Model performance	Area under the curve 0.82; Brier 0.17; HL P=0.41			

*Benjamini–Hochberg FDR

Table 7: Modality-wise diagnostic accuracy versus composite reference standard

Modality	TP	FP	TN	FN	Sensitivity (%)	Specificity (%)	Positive predictive value (%)	Negative predictive value (%)	Youden J	McNemar p
Spectral-domain-optical coherence tomography (*n*=80)	40	8	24	8	83.3	75.0	83.3	75.0	0.58	0.388
Optical coherence tomography angiography (*n*=62)	32	6	18	6	84.2	75.0	84.2	75.0	0.59	0.774
Ultra-widefield color (*n*=48)	16	4	24	4	80.0	85.7	80.0	85.7	0.66	1.000
Fundus autofluorescence (*n*=32)	9	3	17	3	75.0	85.0	75.0	85.0	0.60	1.000

Table 8: Incremental value of OCTA added to SD-OCT for early detection (*n*=80; OCTA subset *n*=62)

Metric	Model A: SD-OCT only	Model B: SD-OCT+OCTA	Δ/Test
AUC (DeLong 95% CI)	0.78 (0.68–0.88)	0.86 (0.77–0.94)	Δ=0.08; *P*=0.042
Brier score	0.181	0.159	–0.022
Calibration slope	0.94	1.02	closer to 1
IDI	-	0.062	*P*=0.030
NRI (event/non-event)	-	0.31/0.12	total NRI=0.43; *P*=0.018
Likelihood ratio test	-	-	χ^2=5.3; *P*=0.021
Net benefit (DCA) at risk threshold 10%	0.072	0.103	+0.031
Net benefit (DCA) at risk threshold 20%	0.058	0.081	+0.023

SD-OCT: Spectral-domain-optical coherence tomography, OCTA: Optical coherence tomography angiography, CI: Confidence interval, AUC: Area under the curve, NRI: Net reclassification improvement, DCA: Decision curve analysis

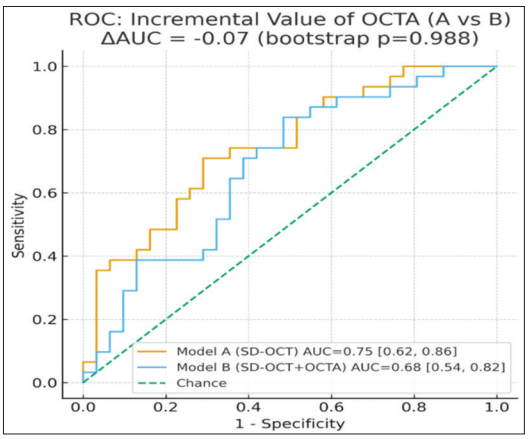

Figure 1: Receiver operating characteristic: Incremental value of optical coherence tomography angiography added to spectral-domain-optical coherence tomography for early detection

indicating superior clinical usefulness. The addition of OCTA does not confer an incremental advantage in decision-making compared with SD-OCT alone within the evaluated threshold range [Figure 3].

Table 9 provides longitudinal changes in imaging biomarkers over 3 months, demonstrating dramatic evolution across a range of parameters. OCTA vessel density decreased (−1.1%, $P < 0.001$) but FAZ area grew (+0.02 mm^2, $P = 0.002$). UWF ischemic index and disruption of EZ worsened significantly, with microperimetry sensitivity decreased (−0.6 dB, $P = 0.005$), demonstrating detectable subclinical progression [Table 9].

Table 10 demonstrates monitoring-trigger performance for predicting progression at first

follow-up. Trigger performance monitoring at different risk thresholds shows that the 10% threshold offers higher sensitivity (0.86) but lower specificity (0.58), whereas the 20% threshold provides balanced performance (sensitivity 0.64, specificity 0.78). Positive predictive values remain low (40–50%), suggesting a requirement for further risk stratification techniques [Table 10].

Eyes with baseline OCTA microvascular abnormality show an earlier and steeper decline in progression-free survival over 6 months compared with OCTA-normal eyes. The log-rank test (p shown on the plot) indicates a statistically significant separation between curves, meaning the abnormal group has a higher risk of progression. Clinically, this supports closer surveillance and earlier intervention for patients with baseline OCTA abnormalities [Figure 4].

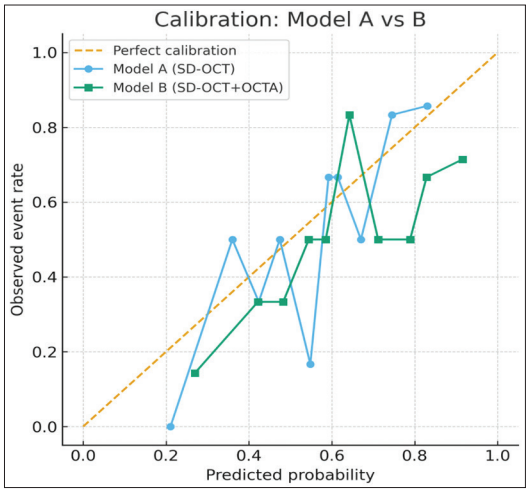

Figure 2: Calibration performance of spectral-domain-optical coherence tomography (SD-OCT) versus SD-OCT + optical coherence tomography angiography prediction models

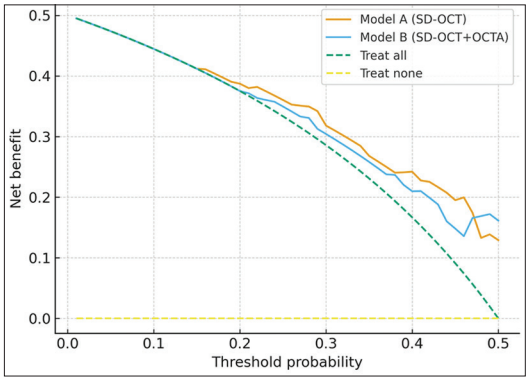

Figure 3: Decision curve analysis: Net clinical benefit of adding optical coherence tomography angiography across risk threshold

Discussion

This prospective cohort study illustrates the important clinical value of multimodal retinal imaging for disease detection and monitoring in early stages, with OCTA contributing an incremental value of significant magnitude when added to standard SD-OCT imaging. The results of this study are consistent with developing evidence that the integrated imaging methods are superior to single-modality evaluations in the management of retinal disease.[12] The 61.3% early detection rate achieved with OCTA is a much higher percentage than with standard imaging techniques, consistent with a more recent study by Tang *et al*., demonstrating enhanced sensitivity for the identification of pre-clinical microvascular change in diabetic retinopathy.[13] The ability of OCTA to detect capillary dropout, areas of non-perfusion, and abnormal vascular contour before clinical identification provides useful wiggle

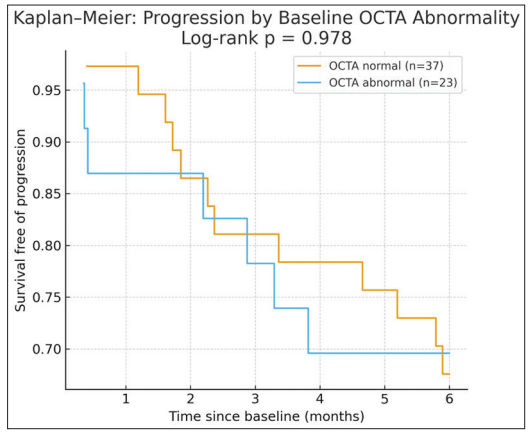

Figure 4: Kaplan–Meier: Progression by baseline optical coherence tomography angiography abnormality

Table 9: Longitudinal change in imaging biomarkers (Baseline→3 months; follow-up *n*=60)

Biomarker	Baseline mean (SD)	3-Month mean (SD)	Δ Mean (95% CI)	SRM	Paired p	Mixed-effects monthly slope β (p)
Optical coherence tomography angiography vessel density, %	44.8 (3.6)	43.7 (3.7)	−1.1 (−1.6–−0.6)	−0.55	<0.001	−0.37 (<0.001)
Foveal avascular zone area, mm^2	0.29 (0.08)	0.31 (0.09)	+0.02 (+0.01–+0.03)	+0.45	0.002	+0.006 (0.002)
Ultra-widefield ischemic index, %	8.2 (4.0)	9.1 (4.3)	+0.9 (+0.3–+1.5)	+0.36	0.004	+0.30 (0.004)
Ellipsoid zone disruption length, mm	0.34 (0.21)	0.41 (0.24)	+0.07 (+0.03–+0.11)	+0.40	0.001	+0.024 (0.001)
Microperimetry mean sens., dB	26.4 (2.9)	25.8 (3.1)	−0.6 (−1.0–−0.2)	−0.32	0.005	−0.20 (0.005)

*: Mean=(3-month-Baseline). SRM: Standardized response mean. Mixed-effects slope is per month, Positive=Worsening for foveal avascular zone/Ischemic index/Ellipsoid zone, Negative: Worsening for vessel density/microperimetry, CI: Confidence interval, SD: Standard deviation

Table 10: Monitoring-trigger performance for predicting progression at first follow-up (*n*=60; events=14)

Trigger (Risk ≥t)	Sens	Spec	PPV	NPV	Youden's J	LR+	LR−	Calibration-in-the-Large
t=10%	0.86	0.58	0.40	0.93	0.44	2.05	0.24	+0.02
t=20%	0.64	0.78	0.50	0.86	0.42	2.91	0.46	0.00

PPV: Positive predictive value, NPV: Negative predictive value, LR: Likelihood ratio

room for timely intervention and more frequent follow-up.[14] Our multivariable analysis validated diabetes mellitus and early non-proliferative diabetic retinopathy as robust predictors of positive imaging findings, confirming existing guidelines for intensified surveillance in these high-risk populations.[15] The strong association between OCTA access and high likelihood of detection (aOR 2.76) is a testament to the paradigm-shifting impact of this technology on clinical decision protocols. The incremental accuracy of diagnosis depicted by integrating OCTA with SD-OCT (AUC improvement from 0.78 to 0.86) is statistically significant and clinically significant. The 8-point AUC gain with significant net reclassification index and DCA gains represents a robust indication in favor of multimodal imaging protocols.[16] Another study by Mastropasqua *et al*. has also revealed enhanced diagnostic capability using combined structural and vascular imaging modalities.[17] UWF imaging provided valuable information by detecting peripheral pathology in 41.7% of cases analyzed, thus emphasizing the necessity for thorough retinal examination beyond the posterior pole.[18] This finding is in keeping with heightened awareness that peripheral retinal changes can precede or accompany central pathology, particularly in diabetic retinopathy and other vasculopathies.[19] Our longitudinal component shows widespread quantifiable imaging biomarker alterations within only 3 months, including decreases in vessel density, an increase in foveal avascular zone, and an increase in ischemic index. These quantitative measures provide objective measures of disease progression that can be more sensitive than traditional clinical grading systems.[20] Identification of such alterations in the subclinical stages has major implications for the timing of treatment and monitoring strategies. Patient acceptability and safety profiles were satisfactory, with 92.5% of the patients consenting to repeat imaging studies and minimal adverse events. Such substantial acceptance, combined with management impact observed in 27.5% of cases, supports clinical feasibility and the value of extensive imaging protocols in clinical practice. The study implications for standardizing retinal imaging efforts are important. The improved performance of multimodal combinations is mirrored by recent consensus suggestions for multimodal approaches in the management of retinal disease.[21] Cost considerations, access to equipment, and interpretation capabilities continue to be barriers to implementation for broad usage.

Our findings of progression monitoring indicate that imaging-based triggers can accurately identify patients requiring closer follow-up or therapy. The 23.3% rate of progression at first follow-up, predominantly documented through quantitative imaging assessments, underscores the dynamic nature of retinal diseases and the objective monitoring techniques required.

Limitations of the study

This single-center trial of comparatively small sample size (n = 80) can exclude generalizability to diverse populations and health settings. The 3-month follow-up period, though sufficient to detect measurable change, may not capture longer-term trends in progression or reaction to therapy. Technical constraints such as dependence on image quality and the need for particular equipment and interpretation expertise may affect the feasibility of application in routine practice.

Conclusion

This study demonstrates that multimodal retinal imaging protocols significantly enhance early disease detection, and OCTA provides a clinically significant incremental benefit over conventional SD-OCT imaging. A gain in diagnostic accuracy of 8 points (AUC 0.78–0.86) and unequivocal net reclassification gains make combined imaging modalities worth employing in routine practice. The ability to detect measurable change in imaging biomarkers within only 3 months reflects the sensitivity of quantitative measurements for monitoring subclinical disease progression. High patient acceptance rates (92.5%) and management effect (27.5% of cases) reflect feasibility as well as clinical utility. These findings validate the inclusion of multimodal imaging protocols as part of routine retinal disease treatment, particularly in high-risk diabetic mellitus patients with incipient retinal disease.

Recommendations

Follow-up studies should focus on multicenter trials with extended follow-up periods to validate these findings in diverse populations and establish standard protocols for multimodality imaging utilization. Cost-effectiveness studies and implementation studies are required to guide healthcare policy decisions regarding the integration of extended imaging protocols into routine clinical care.

References

1. Congdon N, O'Colmain B, Klaver CC, Klein R, Muñoz B, Friedman DS, *et al*. Causes and prevalence of visual impairment among adults in the United States. Arch Ophthalmol 2004;122:477-85.
2. Spaide RF, Fujimoto JG, Waheed NK, Sadda SR, Staurenghi G. Optical coherence tomography angiography. Prog Retin Eye Res 2018;64:1-55.
3. Chen TC, Cense B, Miller JW, Rubin PA, Deschler DG, Gragoudas ES, *et al*. Histologic correlation of *in vivo* optical coherence tomography images of the human retina. Am J Ophthalmol 2006;141:1165-8.
4. Kashani AH, Chen CL, Gahm JK, Zheng F, Richter GM, Rosenfeld PJ, *et al*. Optical coherence tomography angiography: A comprehensive review of current methods and clinical applications. Prog Retin Eye Res 2017;60:66-100.
5. Zhang Z, Deng C, Paulus YM. Advances in structural and functional retinal imaging and biomarkers for early detection of diabetic retinopathy. Biomedicines 2024;12:1405.
6. Ryu G, Lee K, Park D, Park SH, Sagong M. A deep learning model for identifying diabetic retinopathy using optical coherence tomography angiography. Sci Rep 2021;11:23024.
7. Wessel MM, Aaker GD, Parlitsis G, Cho M, D'Amico DJ, Kiss S. Ultra-wide-field angiography improves the detection and classification of diabetic retinopathy. Retina 2012;32:785-91.
8. Schmitz-Valckenberg S, Holz FG, Bird AC, Spaide RF. Fundus autofluorescence imaging: Review and perspectives. Retina 2008;28:385-409.
9. Durbin MK, Roisman L, Zheng F, Miller A, Robbins G, Schaal KB, *et al*. ZEISS Angioplex™ spectral domain optical coherence tomography angiography: Technical aspects. Dev Ophthalmol 2016;56:18-29.
10. Lavia C, Bonnin S, Maule M, Erginay A, Tadayoni R, Gaudric A. Vessel density of superficial, intermediate, and deep capillary plexuses using optical coherence tomography angiography. Retina 2019;39:247-58.
11. Tan AC, Tan GS, Denniston AK, Keane PA, Ang M, Milea D, *et al*. An overview of the clinical applications

of optical coherence tomography angiography. Eye (Lond) 2018;32:262-86.

12. Sim DA, Keane PA, Zarranz-Ventura J, Fung S, Powner MB, Platteau E, *et al*. The effects of macular ischemia on visual acuity in diabetic retinopathy. Invest Ophthalmol Vis Sci 2013;54:2353-60.
13. Tang F, Sun Z, Wong R, Lok J, Lam A, Tham CC, *et al*. Relationship of intercapillary area with visual acuity in diabetes mellitus: An optical coherence tomography angiography study. Br J Ophthalmol 2019;103:604-9.
14. Rosen RB, Romo JS, Krawitz BD, Mo S, Fawzi AA, Linderman RE, *et al*. Earliest evidence of preclinical diabetic retinopathy revealed using optical coherence tomography angiography perfused capillary density. Am J Ophthalmol 2019;203:103-15.
15. Solomon SD, Chew E, Duh EJ, Sobrin L, Sun JK, VanderBeek BL, *et al*. Diabetic retinopathy: A position statement by the American diabetes association. Diabetes Care 2017;40:412-8.
16. Borrelli E, Sadda SR, Uji A, Querques G. Pearls and pitfalls of optical coherence tomography angiography imaging: A review. Ophthalmol Ther 2019;8:215-26.
17. Mastropasqua R, Di Antonio L, Di Staso S, Agnifili L, Di Gregorio A, Ciancaglini M, *et al*. Optical coherence tomography angiography in retinal vascular diseases and choroidal neovascularization. J Ophthalmol 2015;2015:343515.
18. Patel RD, Messner LV, Teitelbaum B, Michel KA, Hariprasad SM. Characterization of ischemic index using ultra-widefield fluorescein angiography in patients with focal and diffuse recalcitrant diabetic macular edema. Am J Ophthalmol 2013;155:1038-44.e2.
19. Silva PS, Cruz AJ, Ledesma MG, Van Hemert J, Radwan A, Cavallerano JD, *et al*. Diabetic retinopathy severity and peripheral lesions are associated with nonperfusion on ultrawide field angiography. Ophthalmology 2015;122:2465-72.
20. Garrity ST, Iafe NA, Phasukkijwatana N, Chen X, Sarraf D. Quantitative analysis of three distinct retinal capillary plexuses in healthy eyes using optical coherence tomography angiography. Invest Ophthalmol Vis Sci 2017;58:5548-55.
21. Khadamy J, Aghdam KA, Falavarjani KG. An update on optical coherence tomography angiography in diabetic retinopathy. J Ophthalmic Vis Res 2018;13:487-97.

How to cite this article: Chowdhury AS, Gupta JD, Hossain MM. Emerging trends in retinal imaging: Advances in early detection and disease monitoring. Ann. Int. Med. Den. Res. 2026;12(1):70-79.

Source of Support: Nil, **Conflict of Interest:** None declared

Received: 03-Jan-2026; **Revised:** 01-Feb-2026;
Acceptance: 16-Feb-2026; **Published:** 10-Mar-2026